One-Pot Synthesis of Superparamagnetic CoO-MCM-41 Nanocomposites with Uniform and Highly Dispersed Magnetic Nanoclusters

Jamal El Haskouri,[a] Saúl Cabrera,[b] Carmen Guillem,[a] Julio Latorre,[a] Aurelio Beltrán,[a] M. Dolores Marcos,[d] Carlos J. Gómez-García,[c] Daniel Beltrán,[a] and Pedro Amorós*[a]

Keywords: Mesoporous materials / Nanocomposites / Superparamagnetism / Nanoparticles / Nanotechnology

Superparamagnetic CoO-MCM-41 mesoporous nanocomposites, with variable cobalt amounts, in the form of well-dispersed CoO-like clusters, were prepared in a large compositional range by a one-step reproducible procedure employing co-hydrolysis and co-condensation of the inorganic precursors in a water/triethanolamine medium.

Introduction

The growing interest on uniform nanometric particles is related to the novel properties associated with systems that are intermediate in size between isolated atoms or molecules and bulk materials.[1] These properties extend the interest in nanostructured materials not only to evident areas, such as microelectronics or catalysis, but also to more original applications, such as the separation of magnetically-labelled biomolecules. In fact, magnetic nanomaterials are currently considered the most promising candidates for data-storage devices, due to the possibility of exploiting the quantum-tunnelling of magnetization effect, which is typical of nanomagnets.[2] Notwithstanding, the special properties of nanoparticulate materials strongly depend on morphological aspects. Control of the size and shape of the particles and the attainment of good dispersity levels are essential requirements.[2] In addition, the use of nanoparticles is limited because of their tendency to form large aggregates, which means that the properties associated with the nanometer range are lost. A well-known solution to overcome this problem consists in the dispersion and/or encapsulation of the nanoparticles in an inert matrix. Indeed, nanosized magnetic materials have been produced by using polymers as a support.[3,4] In this context, silica-based micro- and mesoporous solids, such as zeolites and MCM-41-like materials, are attracting increasing attention as a way to stabilize highly dispersed metal or metal oxide particles.[5] In practice, the functionality of the M41 mesoporous solids has been greatly expanded in recent years by incorporating organic groups or inorganic elements in the pore voids and/or inside the silica walls. Thus, in the search for magnetic materials, a diversity of guest species (semiconductors, metals, metal oxides, clusters, organic molecules, and even single-molecule magnets) have been hosted in the M41 matrices.[6−14] There are relatively few studies concerning Co-containing related materials. These studies are basically focussed on catalytic applications and involve materials in which the cobalt load was carried out after the matrix synthesis.[15−19] As far as we know, there are only two previous publications dealing with the magnetic properties of nanometric cobalt oxides hosted in MCM-41 solids, and, in both cases, the nanocomposites were prepared by post-synthesis impregnation treatments.[20,21] Although soaking really is a common procedure for functionalizing mesoporous silicas, this approach is multistep and, more importantly, frequently leads to necking or even blocking of the pore system.

We report here on a one-pot, reproducible surfactant-assisted procedure yielding superparamagnetic CoO-MCM-

[a] Institut de Ciència dels Materials (ICMUV), Universitat de València,
P. O. Box 2085, 46071 València, Spain
Fax: (internat) + 34-96-3543633
E-mail: pedro.amoros@uv.es
[b] Laboratorio de Sólidos y Química Teórica, Instituto de Investigaciones Químicas UMSA,
Cota-Cota, Calle n° 27, La Paz, Bolivia
E-mail: solidos@megalink.com
[c] Instituto de Ciencia Molecular, Universidad de Valencia,
Doctor Moliner 50, 46100 Burjassot (Valencia), Spain
Fax: (internat) + 34-96-3544859
E-mail: carlos.gomez@uv.es
[d] Departamento de Química, Universidad Politécnica de Valencia,
Camino de Vera s/n, 46071 Valencia, Spain
Fax: (internat) + 34-96-3879349
E-mail: mmarcos@qim.upv.es

41 mesoporous nanocomposites, in which the high dispersion of the CoO-like nanoclusters inside the silica walls is maintained for a high compositional range (up to Si/Co = 23 molar ratio) without blocking of the mesopore system.

Results and Discussion

Mesoporous materials of the MCM-41 type that are rich in CoO-like nanoclusters were synthesized through a one-pot approach using CTABr as a surfactant in a $TEAH_3$–water medium (CTABr = cetyltrimethylammonium bromide; $TEAH_3$ = triethanolamine). The molar ratio of the reagents in the starting solution was 2 Si: *x* Co: 7 $TEAH_3$: 0.50 NaOH/ 0.50 CTABr: 180 H_2O (see Table 1). Our synthesis strategy is based on the use of complexes containing $TEAH_3$ ligands as hydrolytic inorganic precursors. Under basic conditions, and working in an excess of $TEAH_3$, this method unifies the precursor nature (by forming metal-atranes) and it favours the preparation (through co-hydrolysis) of mixed oxides displaying a high chemical homogeneity.[22] Moreover, this approach overcomes, as far as possible, problems related to restrictions on the final stoichiometry. In any case, we should not forget that the replacement of silicon atoms by divalent transition metal cations in a silica matrix is a thermodynamically unfavourable process, and phase segregation must be expected a priori. Thus, the preparative technique is designed to optimize the dispersion of the Co-guest species in the mesoporous host matrix.

EPMA data show that all the samples are chemically homogeneous at micrometric level (spot area about 1μm). Furthermore, only one type of particle morphology, with a hexagonal microstructure that becomes progressively distorted as the Co content increases, is observed in the TEM images of each sample (see Figure 1). Also, the absence of XRD peaks (characteristic of cobalt oxides) at high 2θ values confirms that no extra wall-phase segregation occurs. Hence, at the present scale, which is limited by these techniques, the samples can be considered CoO-MCM-41 monophasic systems. Consequently, the maximum expected dimensions of the possible CoO-like aggregates should be close to the pore-wall size.

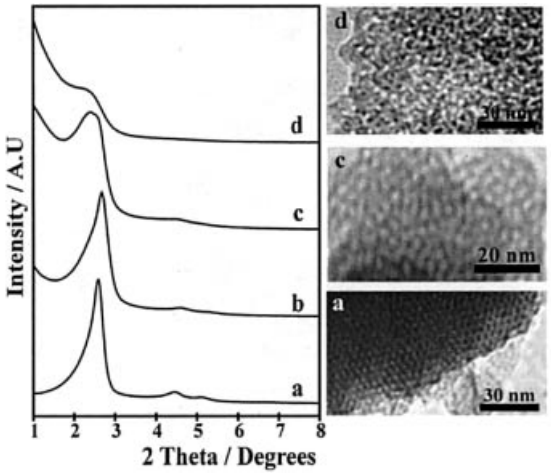

Figure 1. XRD patterns and selected TEM images of CoO-MCM-41 samples; (a) Si/Co = 155; (b) Si/Co = 98; (c) Si/Co = 49; (d) Si/Co = 23

All the samples show XRD patterns that are characteristic for mesoporous hexagonal MCM-41 materials, with at least one strong peak in the low-angle zone and two additional small reflections (exception made of the sample with Si/Co = 23) at higher 2θ values. Nevertheless, the quality and definition of the XRD patterns diminishes as the Co content increases. This evolution indicates progressive lowering of order in the pore array as the cobalt content increases, from ordered hexagonal through disordered hexagonal to wormhole-like systems. The trend is clearly confirmed by the TEM micrographs (see Figure1). Additionally the cell parameter increases with the Co content (see Table 1), an effect typically induced by an effective incorporation of heteroelements in the pore wall of the mesoporous silicas.[23] This behaviour probably results form the interaction of the heteroelement in the growing of the silica network in one-pot (co-hydrolysis) synthesis methods. In our case it could be attributed to a poor charge matching between the CTABr and silica moieties due to the cobalt species, which, in turn, would constitute an indirect probe of the incorporation of cobalt in the pore walls. On the contrary, in mesoporous silicas with metal oxide nanoparticles filling the pores or coating the pore surfaces, prepared through post synthesis treatments, the a_0 value does not significantly depend on the nanoparticle amount.[13,14,17]

Table 1. Co content and selected physical data for CoO-MCM-41

Si/Co (solid)[a]	a_0 [nm][b]	Pore size [nm]	S_{BET} [$m^2\ g^{-1}$]	Pore-wall thickness [nm]
155	3.80	2.50	908.5	1.30
98	3.80	2.48	662.0	1.32
49	4.09	2.47	526.3	1.63
23	4.14	2.50	478.6	1.64

[a] Values averaged from the EPMA of about 40 different particles. [b] Calculated cell parameters assuming an MCM-41 type hexagonal cell.

The loss of X-ray intensity observed in the XRD, corresponding to the solid with the highest Co content, must be attributed to a significant loss of order more than to phase-cancellation phenomena, which are associated with the introduction of scattering material into the pores or to a partial collapse of the mesostructure. In fact, as indicated above, the observation by TEM of a single type of particle of homogeneous morphology containing mesopores allows us to discard the presence of collapsed bulk materials.

Mesoporosity is evaluated by N_2 adsorption−desorption isotherms (see Figure 2). All the curves display one well-defined step at intermediate P/P_0 values typical of type IV isotherms. Although incorporation of Co results in a gradual decrease of the surface area, the high surface area and porosity, characteristic of the MCM-41 silica, are retained in all cases. Moreover, the fact that the pore size remains practically constant as the cobalt content increases, together with the absence of significant hysteresis loops in the isotherms, indicates that no necking or blocking of the pore system occurs. The thickness of the pore walls (estimated from XRD and porosity data) increases with the Co content, which explains the decrease of the S_{BET}. Thus, it is reasonable to propose that CoO nanoclusters are incorporated into the silica walls.

The UV/Vis spectra of some selected CoO-MCM-41 samples dehydrated at 400 °C are shown in Figure 3. All the spectra display a strong absorption in the visible region

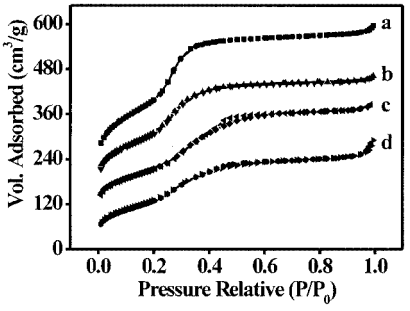

Figure 2. N_2 adsorption−desorption isotherms (curves are shifted for clarity) of CoO-MCM-41 samples; (a) Si/Co = 155; (b) Si/Co = 98; (c) Si/Co = 49; (d) Si/Co = 23

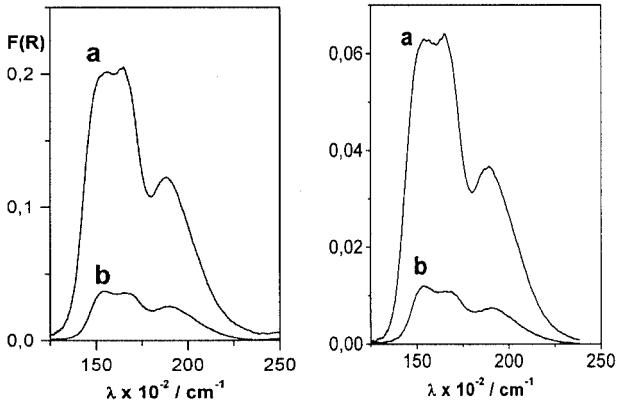

Figure 3. UV/Vis spectra of CoO-MCM-41 Si/Co = 23 (left) and Si/Co = 98 (right); (a) dehydrated sample; (b) hydrated sample

(15000−20000 cm^{-1}) with three maxima at around 15000, 17000 and 19000 cm^{-1}. This triplet can be unambiguously assigned to the $^4A_2(F) \rightarrow {}^4T_1(P)$ transition of cobalt(II) ions in tetrahedral oxygen environments, which allows us to discard the presence of Co^{III} atoms. In all cases, the characteristic blue colour of the materials is typical of tetrahedral $Co^{II}O_4$ sites. The intensity of this band significantly decreases with hydration, and it recovers reversibly by posterior drying. This behaviour clearly indicates that a certain proportion of the tetrahedral cobalt atoms becomes octahedrally coordinated by water uptaking and lies on the surface of the pore wall. Taking into account the large difference between the absorption molar coefficients of the bands due to electronic transitions associated to octahedral vs. tetrahedral Co^{II} sites, it can be reasonably assumed that the area under the vis curve is proportional to the number of non-hydrated tetrahedral cobalt centres. With this simplification, we can estimate the ratio of "surface" (water accessible)-to-"bulk" (inaccessible) Co ions by the intensity variation of the band after hydration. Remarkably, this ratio is practically constant and close to 2:7, irrespective of the cobalt content in the sample. This result strongly suggests that the nature of the CoO clusters does not depend on the Co concentration in the sample and supports the existence of a regular interaction of the clusters with the pore walls that become progressively distorted by increasing the cluster concentration.

The results of the magnetic measurements offer definitive evidence for the fact that the particle size remains constant, independent of the Si/Co molar ratio. Thus, all the samples show identical behaviour: (i) a sharp increase of the DC magnetic susceptibility below 12−17 K; (ii) a frequency-dependent AC signal with maxima at 4−7 K in the in-phase signal (χ') and at 3−5 K in the out-of-phase signal (χ''; see Figure 4); (iii) deviations in the zero-field-cooled and field-cooled susceptibilities below 10−15 K, with a remnant magnetization that vanishes at around 15 K for all the samples; and (iv) hysteresis cycles in the isothermal magnetization at low temperatures. All these features suggest a superparamagnetic behaviour with a blocking temperature

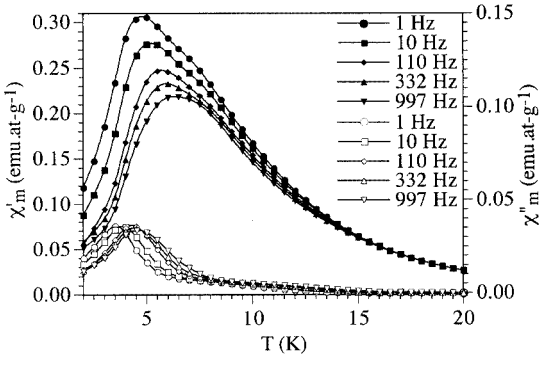

Figure 4. Thermal variation of χ' (filled symbols, scale on the left) and χ'' (empty symbols, scale on the right) at different frequencies for the sample with Si/Co = 49

Table 2. CoO particle size determined from magnetic measurements

Si/Co (solid)	T_B [K][a]	E_a [K]	D [nm][b]
155	13	123.1	2.0
49	14	107.2	1.9
23	16	105.8	1.9

[a] Defined as the temperature at which $\chi'' \neq 0$. [b] Diameter determined from the E_a data ($E_a = K \cdot V$).

of around 15 K (see Table 2). It should be noted that possible spin-glass behaviour is excluded since the conditions for a spin-glass system are not fulfilled and the activation energies obtained from the frequency dependence of the maxima in χ'' (see below) are much lower than those expected for spin-glass systems.[19]

A way of estimating the particle size is to use the relationship between the activation energy of the blocking process of the resultant moments on the particles (E_a) and the particle volume (V), that is, $E_a = K \cdot V$, where K is the energy density of the magnetic anisotropy.[17] With the activation energies (E_a ca. 90−120 K, see Table 2) obtained from the Arrhenius law for the temperatures of the maxima in χ'' (T_m) as a function of the frequency (ν), $\nu = \nu_0 \cdot \exp(-E_a/kBT_m)$, and taking $K = 3.8 \cdot 10^6$ erg·cm^{-3},[20] we can estimate that the particle sizes are between 1.8 and 2.0 nm (see Table 2).

In any case, the relevant conclusion from the magnetic and spectroscopic studies is that, regardless of the Si/Co ratio, the CoO particles are similar and homo-disperse with sizes close to 2 nm. Assuming that the structure is sphalerite, these nanoclusters should contain around 200 CoO units. Taking the "nonaccessible"-to-"accessible" Co ratio found by spectroscopy into account, we postulate a model for these CoO-MCM-41 nanocomposites in which the CoO nanodomains are partially embedded (about 25 %) in the silica matrix.

Conclusion

In summary, we present a simple one-pot surfactant-assisted approach for obtaining superparamagnetic mesoporous materials with high cobalt content and well-dispersed uniform CoO nanoparticles within the inorganic walls, without blocking of the pore system. The homogeneity in size, nature and dispersion of the CoO nanoparticles can be explained by the fact that the growing process of the nucleated CoO species, generated by the hydrolysis of the Co precursor, is blocked by the relatively slower condensation of the mesostructured silica network. In short (in the experimental Si/Co concentrations) the time consumption for the nucleation and growing of the CoO particles is constant and limited by the silica polymerisation process. These materials may be described as nanocomposites of CoO clusters on mesoporous silicas. The nanometric organization of highly dispersed and accessible CoO nanodomains could be of catalytic interest in Fischer−Tropsch and ODH processes.

Experimental Section

CoO-MCM-41 Mesoporous Nanocomposites: The molar ratio of the reagents in the starting solution was 2 Si: x Co: 7 $TEAH_3$: 0.50 NaOH/ 0.50 CTABr: 180 H_2O (Table 1). In a typical synthesis leading to the Si/Co = 49 mesoporous material, 0.49 g of NaOH were dissolved at 60 °C in 20 mL of $TEAH_3$. After a few minutes, 10.5 mL of TEOS and 0.20 g of $CoCl_2$ were added whilst stirring, and the mixture was heated at 150 °C for 5 min. The resulting solution was cooled down to 100 °C, and 4.68 g of CTABr were added while stirring. Then, 80 mL of water were added with vigorous stirring at 60 °C. After a few minutes, a pale-blue suspension resulted, and it was aged at room temperature for 24 hours. The resulting powder was filtered off, washed with water and ethanol, and air dried. Finally, to open the mesopore system, the surfactant was removed by calcination at 550 °C in the course of 5 hours under air atmosphere.

All samples were analyzed and characterized by electron probe microanalysis (EPMA, Philips SEM-515), XRD techniques (Seifert 3000TT diffractometer; Cu-K_α radiation), TEM (Philips CM10 microscope), N_2 adsorption−desorption isotherms (Micromeritics ASAP2010), UV/Vis spectroscopy (UV-250 1PC Shimadzu), magnetic susceptibility measurements (DC and AC magnetic fields) and isothermal magnetization (PPMS-9 and SQUID susceptometer MPMS-XL-5, Quantum Design).

Acknowledgments

This research was supported by the Spanish Ministerio de Ciencia y Tecnología under grants MAT2000-1387-C021 and MAT2002-04239-C03-02. J. E. H. thanks the Spanish Ministerio de Educación y Ciencia for a post-doctoral grant.

[1] A. P. Alivisatos, *Science* **1996**, *271*, 933−937.
[2] T. Hyeon, *Chem. Commun.* **2003**, 927−934, and references cited therein.
[3] I.-W. Park, M. Yoon, Y. M. Kim, Y. Kim, H. Yoon, H. J. Song, V. Volkov, A. Avilov, Y. J. Park, *Solid State Commun.* **2003**, *126*, 385−389.
[4] J. Ramos, A. Millán, F. Palacio, *Polymer* **2000**, *41*, 8461−8464.
[5] F. Schüth, A. Wingen, J. Sauer, *Microporous Mesoporous Mater.* **2001**, *44*, 465−476.
[6] C. Yang, H.-S. Sheu, K.-J. Chao, *Adv. Funct. Mater.* **2002**, *12*, 143−148.
[7] N. R. B. Coleman, M. A. Morris, T. P. Spakling, J. D. Holmes, *J. Am. Chem. Soc.* **2001**, *123*, 187−188.
[8] F. Gao, Q. Lu, X. Llu, Y. Yan, D. Zhao, *Nano Lett.* **2001**, *1*, 743−748.
[9] T. Coradin, J. Larionova, A. A. Smith, G. Rogez, R. Clérac, C. Guérin, G. Blondin, R. E. P. Winpenny, C. Sanchez, T. Mallah, *Adv. Mater.* **2002**, *14*, 896−898.
[10] K. Moller, T. Bein, *Chem. Mater.* **1998**, *10*, 2950−2963, and references cited therein.
[11] A. Jentys, N. H. Pham, H. Vinek, M. Englisch, J. A. Lercher, *Microporous Mater.* **1996**, *6*, 13−17.
[12] S. Murray, M. Trudeau, D. M. Antonelli, *Adv. Mater.* **2000**, *12*, 1339−1342.
[13] R. Köhn, D. Paneva, M. Dimitrov, T. Tsoncheva, I. Mitov, C. Minchev, M. Fröba, *Microporous Mesoporous Mater.* **2003**, *63*, 125−137.
[14] R. Köhn, M. Fröba, *Catal. Today* **2001**, *68*, 227−236.

[15] A. F. Gross, M. R. Diehl, K. C. Beverly, E. K. Richman, S. H. Tolbert, *J. Phys. Chem. B* **2003**, *107*, 5475−5482.
[16] S. Suvanto, J. Hukkamäki, T. T. Pakkanen, T. A. Pakkanen, *Langmuir* **2000**, *16*, 4109−4115.
[17] M. Wei, K. Okabe, H. Arakawa, Y. Teraoka, *New. J. Chem.* **2002**, *26*, 20−23.
[18] D. Yin, W. Li, W. Yang, H. Xiang, Y. Sun, B. Zhing, S. Peng, *Microporous Mesoporous Mater.* **2001**, *47*, 15−24.
[19] A. Vinu, J. Dedecek, V. Murugesan, M. Hartmann, *Chem. Mater.* **2002**, *14*, 2433−2435.
[20] M. Sato, S. Takada, S. Kohiki, T. Babasaki, H. Deguchi, M. Oku, M. Mitome, *Appl. Phys. Lett.* **2000**, *77*, 1194−1196.
[21] S. Takada, M. Fujii, S. Kohiki, T. Babasaki, H. Deguchi, M. Mitome, M. Oku, *Nano Lett.* **2001**, *1*, 379−382.
[22] S. Cabrera, J. El Haskouri, C. Guillem, J. Latorre, A. Beltrán, D. Beltrán, M. D. Marcos, P. Amorós, *Solid State Sci.* **2000**, *2*, 405−420.
[23] A. Sayari, *Chem. Mater.* **1996**, *8*, 248−257.
[24] J. A. Mydosh "*Spin Glasses: an Experimental Introduction*", Taylor and Francis, London, **1993**.
[25] M. Gruyters, *J. Magn. Magn. Mater.* **2002**, *248*, 248−257.

Received December 1, 2003

